Chin. J. Astron. Astrophys. Vol. 2 (2002), No. 3, 197–206
(http://www.chjaa.org or http://chjaa.bao.ac.cn)

Chinese Journal of
Astronomy and
Astrophysics

Positions and Spectral Energy Distributions of 41 Star Clusters in M33

Jun Ma*, Xu Zhou, Jian-Sheng Chen, Hong Wu, Zhao-Ji Jiang, Sui-Jian Xue and Jin Zhu

National Astronomical Observatories, Chinese Academy of Sciences, Beijing 100012

Received 2002 January 3; accepted 2002 March 9

Abstract We present accurate positions and multi-color photometry for 41 star clusters detected by Melnick & D'odorico in the nearby spiral galaxy M33 as a part of the BATC Color Survey of the sky in 13 intermediate-band filters from 3800 to 10 000 Å. The coordinates of the clusters are found from the HST Guide Star Catalog. By aperture photometry, we obtain the spectral energy distributions of the clusters. Using the relations between the BATC intermediate-band system and *UBVRI* broadband system, we derive their V magnitudes and $B-V$ colors and find that most of them are blue, which is consistent with previous findings.

Key words: galaxies: individual (M33) — galaxies: evolution — galaxies: star clusters

1 INTRODUCTION

Hubble did the pioneer work in the discovering of star clusters in M33. He detected 18 diffuse objects and showed that these objects were quite different from the globular clusters of M31: Hubble found that these objects of M33 are about 1.5 magnitudes fainter, and that the brightest and best investigated ones are bluer (see details from Sharov & Lyutyi 1984). Before 1982, there are only a few dozen cluster candidates in M33 known. Christian & Schommer (1982) detected more than 250 non-stellar objects using 14×14 inch^2 unfiltered, unbaked, IIa-O focus plate exposed for 150 minutes with the Kitt Peak 4 m Richey-Chrétien (R-C) direct camera. Recently, Chandar, Bianchi & Ford (1999, 2001) discovered 168 star clusters from 55 deep *Hubble Space Telescope* (HST) WFPC2 fields from their program and the HST archive, 130 of which were previously unknown. We should emphasize that the high spatial resolution of HST images can guarantee the identification of star clusters from their shape (see details from Chandar, Bianchi & Ford 1999). Most candidate clusters detected from the ground-based work lie in the outskirts of the parent galaxy, while the HST images allowed Chandar, Bianchi & Ford (1999, 2001) to penetrate into the crowded, spiral regions of M33.

* E-mail: majun@vega.bac.pku.edu.cn

The importance of the study of star clusters can hardly be overstated, especially in the Local Group galaxies. Star clusters, which represent, in distinct and luminous "packets", single age and single abundance points, and encapsulate at least a partial history of the parent galaxy's evolution, can provide a unique laboratory for studying the global properties of the parent galaxy.

M33 is a small Scd Local Group galaxy, about 15 times farther from us than the LMC (distance modulus 24.64) (Freedman, Wilson & Madore 1991; Chandar, Bianchi & Ford 1999). It is interesting and important because it represents a morphological type intermediate between the largest "early-type" spirals and the dwarf irregulars in the Local Group (Chandar, Bianchi & Ford 1999). Moreover, at a distance of $\sim$ 840 kpc, M33 is the only nearby late-type spiral galaxy, so it can provide an important link between the cluster populations of earlier-type spirals (Milky Way galaxy and M31) and the numerous, nearby later-type dwarf galaxies. For example, using 157 HST/WFPC2 images of M31, Barmby & Huchra (2001) found 82 previously cataloged globular cluster candidates as well as 32 new globular cluster candidates, and estimated the total number of such objects in M31 as 460 ± 70. In contrast, Schommer et al. (1991) estimated the total number of "true" globular cluster population of M33 to be only $\sim$ 20. What is the reason for such a large difference in the number of globular clusters for these two nearby spiral galaxies? It should be mentioned that Chandar, Bianchi & Ford (2001)'s estimate of the total number of globular clusters in M33 is higher at 75 ± 14.

M33 was observed as part of the galaxy calibration program of the Beijing-Arizona-Taiwan-Connecticut (BATC) Multicolor Sky Survey (Fan et al. 1996; Zheng et al. 1999) from 1995 September 23 to 2000 August 28. This program uses the 60/90 cm Schmidt telescope at the Xinglong Station of Beijing Astronomical Observatory (BAO), and has a custom designed set of 15 intermediate-band filters to do spectrophotometry on pre-selected 1 deg^2 regions of the northern sky. The BAO Schmidt telescope is equipped with a Ford 2048×2048 Ford CCD at its main focus. Using the 13 intermediate-band filters images of M33 obtained from the BATC Multicolor Sky Survey, Ma et al. (2001) studied the 57 star clusters of Chandar et al. (1999), and obtained their spectral energy distributions (SEDs) by aperture photometry, and estimated their ages by comparing the integrated photometric measurements with theoretical stellar population synthesis models of the clusters.

In this paper, we locate the coordinates of the sample clusters (Melnick & D'odorico, 1978) using the HST Guide Star Catalog, and obtain their SEDs by aperture photometry. Details of the observation and data reduction are given in Section 2 and a summary is given in Section 3.

2 SAMPLE OF STAR CLUSTERS, OBSERVATIONS AND DATA REDUCTION

2.1 Sample of Star Clusters

The sample of star clusters in this paper is from Melnick & D'Odorico (1978), who detected 58 stellar clusters in M33. Melnick & D'Odorico (1978) selected all objects brighter than $m(B) \simeq 19.5$ magnitudes that appeared clearly non-stellar on a baked IIIa-J+GG385 plate. This plate, which covered a field of about one degree in diameter, was exposed for 4 hours with the 1.52 m Ritchey-Chretien telescope (f/8.75) at the Palomar Observatory. All objects selected were then cross-checked using the H_α map of Boulesteix et al. (1974) to eliminate emission line objects. The remaining objects were then re-examined on the blue, visual and H_α plates of M33 from the 1.82 m Asiago telescope collection. The authors had a final list of 58 cluster candidates, which they marked on the plate. However, they did not give the coordinates of these clusters. In this paper, we will give their coordinates using the HST Guide Star Catalog.

Figure 1 shows the image of M33 in filter BATC07 (5785 Å), the circles mark the positions of the sample clusters of (Melnick & D'odorico, 1978). Clusters 51 and 58 are outside our images.

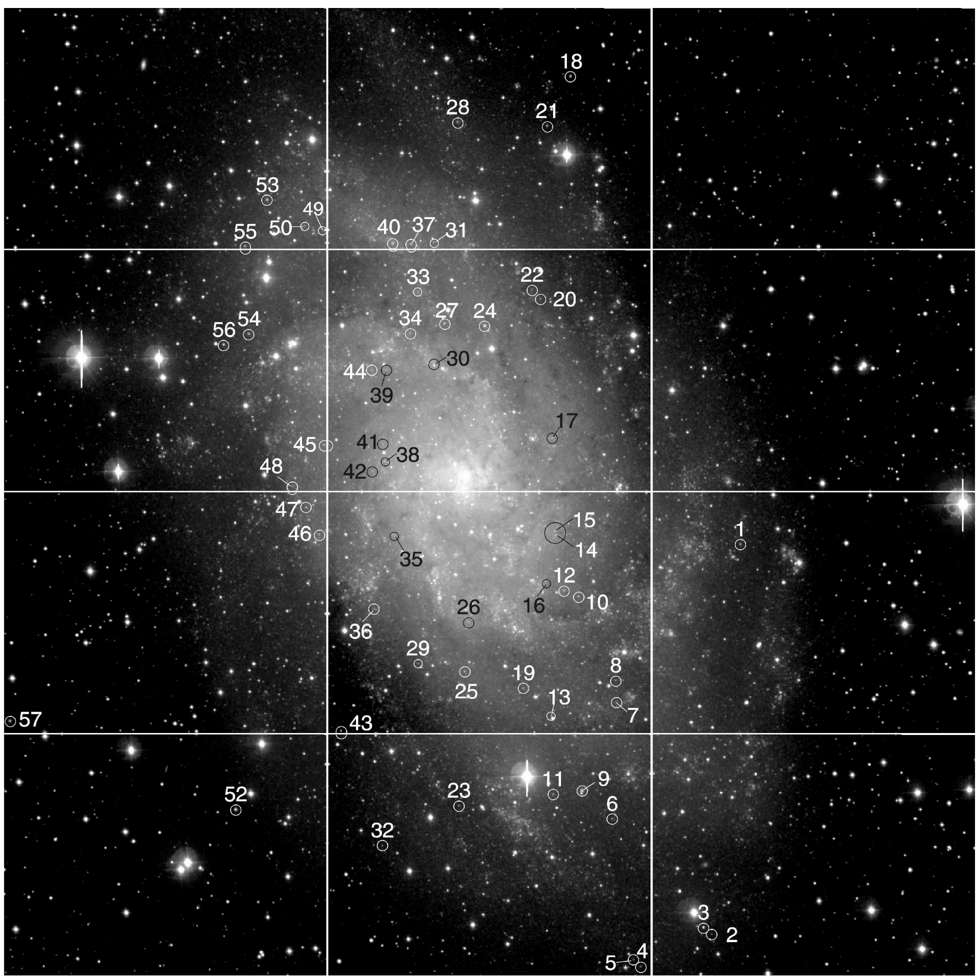

Fig. 1 M33 in filter BATC07 (5785 Å) and the positions of the sample star clusters. The center of the image is RA = $01^h33^m50.58^s$, Decl.= $30°39'08.4''$ (J2000.0). North is up and east is to the left.

2.2 Observations and Data Reduction

Our large-field, multi-color observations of the spiral galaxy M33 were obtained in the BATC photometric system. The multi-color BATC filter system, which was specifically designed to avoid contamination from the brightest and most variable night sky emission lines, comprises

15 intermediate-band filters, covering the total optical wavelength range from 3000 to 10 000 Å. The images of M33 covering the whole optical body of M33 were accumulated in 13 intermediate band filters with a total exposure time of about 32.75 hours from 1995 September 23 to 2000 August 28. The dome flat-field images were taken by using a diffuse plate in front of the correcting plate of the Schmidt telescope. For flux calibration (see Zhou et al. 2001; Yan et al. 1999 for a detail), the Oke-Gunn primary flux standard stars HD19445, HD84937, BD+262606 and BD+174708 were observed during photometric nights. *Column* 6 in Table 1 gives the calibration error, in magnitudes, for the standard stars in each filter. The formal errors we obtained for these stars in the 13 BATC filters are $\lesssim$ 0.02 mag. This indicates that we can define the standard BATC system to an accuracy of $\lesssim$ 0.02 mag.

Table 1 Parameters of the BATC Filters and Statistics of Observations

No.	Name	cw[a] (Å)	Exp. (hr)	N.img[b]	rms[c]
(1)	(2)	(3)	(4)	(5)	(6)
1	BATC03	4210	00:55	04	0.024
2	BATC04	4546	01:05	04	0.023
3	BATC05	4872	03:55	19	0.017
4	BATC06	5250	03:19	15	0.006
5	BATC07	5785	04:38	17	0.011
6	BATC08	6075	01:26	08	0.016
7	BATC09	6710	01:09	08	0.006
8	BATC10	7010	01:41	08	0.005
9	BATC11	7530	02:07	10	0.017
10	BATC12	8000	03:00	11	0.003
11	BATC13	8510	03:15	11	0.005
12	BATC14	9170	01:15	05	0.011
13	BATC15	9720	05:00	26	0.009

[a] Central wavelength for each BATC filter; [b] Image numbers for each BATC filter;
[c] Calibration error, in magnitude, for each filter as obtained from the standard stars.

The data were reduced with standard procedures, including bias subtraction and flat-fielding of the CCD images, with an automatic data reduction software named PIPELINE I developed for the BATC multi-color sky survey (see Ma et al. 2001, 2002a for a detail).

2.3 Coordinates of Star Clusters

By comparing Figure 1 of Melnick & D'Odorico (1978) with our Xionglong Schmidt image, we obtain the coordinates of the clusters listed in Table 2. In the course of the work, we noticed that some clusters were common to Melnick & D'Odorico (1978) and Chandar, Bianchi & Ford (1999, 2001), namely, clusters 11, 12, 14, 15, 17, 20, 22, 24, 25, 26, 30, 42, 47, 48, and 55 in Melnick & D'Odorico (1978) are, respectively, clusters 114, 16, 151, 150, 90, 110, 112, 61, 104, 4, 33, 55, 70, 72, and 81 in Chandar, Bianchi & Ford (1999, 2001). The coordinates of these have been given by Chandar, Bianchi & Ford (1999, 2001) and their SEDs have been obtained by Ma et al. (2001, 2002a, 2002b).

Table 2 Properties of 41 Star Clusters

Cluster (1)	R.A. (J2000) (2)	Decl. (J2000) (3)	V (BATC) (4)	$B-V$ (BATC) (5)
1	01:32:42.94	30:35:38.5	17.661 ± 0.025	0.061 ± 0.035
2	01:32:52.67	30:14:31.3	18.805 ± 0.067	–0.044 ± 0.085
3	01:32:54.68	30:14:54.2	16.565 ± 0.015	0.908 ± 0.026
4	01:33:09.83	30:12:51.2	18.736 ± 0.047	–0.064 ± 0.065
5	01:33:11.66	30:13:14.9	18.737 ± 0.047	0.858 ± 0.097
6	01:33:16.08	30:20:57.1	18.287 ± 0.047	0.029 ± 0.063
7	01:33:14.28	30:27:11.2	18.866 ± 0.087	0.123 ± 0.110
8	01:33:14.30	30:28:22.9	18.374 ± 0.055	0.686 ± 0.102
9	01:33:23.43	30:22:31.4	16.442 ± 0.012	1.089 ± 0.026
10	01:33:23.10	30:33:00.8	17.408 ± 0.038	–0.004 ± 0.048
13	01:33:30.68	30:26:32.2	17.819 ± 0.040	0.614 ± 0.070
16	01:33:31.14	30:33:46.0	18.159 ± 0.254	0.072 ± 0.297
18	01:33:21.87	31:01:10.7	17.115 ± 0.017	1.280 ± 0.036
19	01:33:37.55	30:28:05.3	17.703 ± 0.051	–0.021 ± 0.067
21	01:33:28.08	30:58:30.4	17.824 ± 0.028	0.788 ± 0.050
23	01:33:54.38	30:21:52.6	18.584 ± 0.059	0.339 ± 0.091
27	01:33:55.12	30:47:58.0	16.571 ± 0.022	0.092 ± 0.029
28	01:33:50.65	30:58:49.9	17.513 ± 0.029	0.046 ± 0.038
29	01:34:03.82	30:29:34.1	18.439 ± 0.092	0.126 ± 0.121
31	01:33:57.34	30:52:17.9	17.968 ± 0.050	0.070 ± 0.065
32	01:34:13.81	30:19:47.9	18.353 ± 0.043	0.098 ± 0.064
33	01:34:01.66	30:49:43.8	17.882 ± 0.074	0.096 ± 0.103
34	01:34:03.85	30:47:29.2	17.581 ± 0.065	0.122 ± 0.082
35	01:34:08.93	30:36:34.2	17.652 ± 0.091	–0.152 ± 0.110
36	01:34:14.62	30:32:35.7	18.082 ± 0.070	0.086 ± 0.098
37	01:34:03.06	30:52:13.7	16.869 ± 0.023	0.078 ± 0.031
38	01:34:10.90	30:40:30.1	17.798 ± 0.090	0.222 ± 0.122
39	01:34:10.08	30:45:29.7	17.566 ± 0.058	0.005 ± 0.077
40	01:34:07.67	30:52:17.9	16.876 ± 0.043	–0.027 ± 0.057
41	01:34:11.31	30:41:28.0	18.163 ± 0.208	0.173 ± 0.279
43	01:34:23.47	30:25:58.9	17.834 ± 0.031	0.032 ± 0.045
44	01:34:13.80	30:45:31.4	17.812 ± 0.100	0.214 ± 0.132
45	01:34:25.36	30:41:28.8	17.478 ± 0.030	0.395 ± 0.044
46	01:34:27.10	30:36:42.8	17.737 ± 0.041	0.168 ± 0.060
49	01:34:24.40	30:53:05.5	18.039 ± 0.041	0.563 ± 0.075
50	01:34:29.09	30:53:20.7	18.363 ± 0.082	0.318 ± 0.125
52	01:34:49.59	30:21:56.0	16.151 ± 0.010	0.434 ± 0.017
53	01:34:38.35	30:54:49.2	16.901 ± 0.018	0.957 ± 0.034
54	01:34:43.70	30:47:38.0	17.185 ± 0.024	0.190 ± 0.034
56	01:34:50.07	30:47:04.1	16.495 ± 0.014	0.050 ± 0.019
57	01:35:45.70	30:26:53.9	17.243 ± 0.018	0.664 ± 0.032

2.4 Integrated Photometry

For each star cluster, the PHOT routine in DAOPHOT (Stetson 1987, 1992) was used to acquire its magnitudes. To avoid contamination from nearby objects, a smaller aperture of

6.8″, which corresponds to a diameter of 4 pixels in Ford CCDs, was adopted. The aperture corrections were computed using isolated stars. Finally, the spectral energy distributions of 41 star clusters in 13 BATC filters were obtained. Table 3 contains the following information: *Column 1* is cluster number which is taken from Melnick & D'odorico (1978). *Column* 2 to *Column* 14 show the magnitudes in the different bands and the second line of each entry gives the corresponding uncertainties. The uncertainties for each filter are given by DAOPHOT.

Table 3 SEDs of 41 Star Clusters

No.	03	04	05	06	07	08	09	10	11	12	13	14	15
(1)	(2)	(3)	(4)	(5)	(6)	(7)	(8)	(9)	(10)	(11)	(12)	(13)	(14)
1	17.792	17.609	17.616	17.567	17.579	17.495	17.422	17.383	17.338	17.309	17.357	17.215	17.200
	0.021	0.016	0.016	0.017	0.014	0.016	0.016	0.018	0.018	0.018	0.033	0.024	0.047
2	18.872	18.669	18.795	18.673	18.752	18.693	18.688	18.570	18.775	18.763	18.911	18.682	19.340
	0.039	0.036	0.033	0.040	0.040	0.044	0.042	0.049	0.069	0.064	0.119	0.108	0.403
3	18.151	17.156	17.059	16.724	16.318	16.144	15.933	15.728	15.724	15.672	15.798	15.561	15.598
	0.027	0.013	0.012	0.013	0.008	0.008	0.007	0.008	0.007	0.007	0.010	0.009	0.013
4	18.770	18.597	18.766	18.572	18.696	18.632	18.716	18.589	18.731	18.775	18.945	18.819	18.810
	0.038	0.030	0.027	0.028	0.027	0.034	0.034	0.039	0.043	0.058	0.098	0.087	0.147
5	20.012	19.327	19.139	18.712	18.572	18.384	18.152	17.930	17.986	17.823	17.897	17.668	17.652
	0.112	0.052	0.036	0.035	0.026	0.031	0.024	0.028	0.027	0.030	0.052	0.037	0.058
6	18.438	18.221	18.346	18.137	18.229	18.141	18.158	18.057	18.170	18.194	18.187	18.201	18.209
	0.034	0.029	0.025	0.029	0.028	0.030	0.032	0.041	0.047	0.048	0.072	0.075	0.107
7	18.857	18.793	17.574	18.917	18.824	18.969	17.187	18.628	18.583	18.696	18.785	17.914	18.477
	0.055	0.052	0.016	0.060	0.048	0.061	0.019	0.071	0.078	0.090	0.151	0.067	0.181
8	19.191	18.872	18.675	18.418	18.210	18.092	17.881	17.789	17.801	17.725	17.697	17.540	17.611
	0.083	0.058	0.043	0.043	0.031	0.031	0.029	0.031	0.033	0.036	0.048	0.042	0.066
9	17.991	17.205	16.856	16.426	16.265	16.060	15.852	15.660	15.614	15.489	15.480	15.321	15.189
	0.026	0.015	0.010	0.009	0.007	0.007	0.007	0.007	0.007	0.006	0.007	0.007	0.009
10	17.476	17.313	17.396	17.326	17.340	17.297	17.265	17.235	17.240	17.211	17.179	17.154	17.295
	0.022	0.021	0.021	0.024	0.022	0.024	0.027	0.031	0.038	0.037	0.047	0.045	0.074
13	18.751	18.232	18.178	17.609	17.764	17.622	17.457	17.319	17.123	17.154	17.207	17.167	16.908
	0.058	0.037	0.036	0.024	0.024	0.025	0.022	0.023	0.026	0.026	0.041	0.034	0.052
16	18.321	18.111	18.114	18.000	18.123	18.072	18.299	18.161	18.204	18.154	18.524	18.706	18.369
	0.100	0.092	0.177	0.093	0.163	0.189	0.299	0.228	0.261	0.226	0.384	0.429	0.410
18	18.763	18.047	17.526	17.219	16.945	16.875	16.640	16.584	16.417	16.168	16.081	16.071	15.797
	0.036	0.020	0.014	0.013	0.010	0.010	0.009	0.010	0.009	0.008	0.012	0.010	0.014
19	17.715	17.599	17.676	17.629	17.637	17.608	17.552	17.458	17.531	17.464	17.461	17.318	17.327
	0.028	0.031	0.029	0.031	0.030	0.034	0.036	0.038	0.046	0.044	0.056	0.056	0.068
21	18.948	18.358	18.138	17.939	17.655	17.599	17.420	17.396	17.223	17.083	16.990	16.967	16.798
	0.047	0.026	0.020	0.021	0.016	0.017	0.014	0.018	0.015	0.016	0.026	0.018	0.042
23	19.079	18.783	18.779	18.549	18.497	18.461	18.393	18.262	18.248	18.282	18.214	18.251	18.370
	0.062	0.047	0.036	0.037	0.035	0.037	0.039	0.042	0.047	0.048	0.081	0.070	0.112
27	16.764	16.563	16.649	16.570	16.490	16.503	16.468	16.450	16.420	16.369	16.366	16.304	16.320
	0.015	0.013	0.013	0.014	0.013	0.014	0.015	0.016	0.020	0.020	0.023	0.024	0.032
28	17.579	17.474	17.530	17.510	17.475	17.575	17.575	17.606	17.596	17.563	17.486	17.486	17.331
	0.020	0.017	0.016	0.019	0.017	0.019	0.020	0.025	0.026	0.027	0.047	0.032	0.058

Table 3 Continued

No.	03	04	05	06	07	08	09	10	11	12	13	14	15
(1)	(2)	(3)	(4)	(5)	(6)	(7)	(8)	(9)	(10)	(11)	(12)	(13)	(14)
29	18.660	18.456	18.503	18.363	18.409	18.453	18.389	18.229	18.129	18.217	18.346	17.890	18.083
	0.059	0.054	0.051	0.061	0.051	0.067	0.069	0.070	0.071	0.083	0.128	0.072	0.139
31	18.185	17.920	17.987	17.965	17.936	18.048	18.079	18.092	18.111	18.022	18.003	18.019	18.040
	0.034	0.029	0.026	0.030	0.029	0.034	0.042	0.050	0.057	0.066	0.081	0.095	0.133
32	18.607	18.332	18.404	18.273	18.294	18.272	18.179	18.050	17.973	18.045	18.133	17.928	18.139
	0.044	0.032	0.026	0.026	0.025	0.029	0.026	0.035	0.029	0.039	0.066	0.054	0.110
33	18.016	17.876	17.891	17.840	17.819	17.829	17.823	17.814	17.770	17.649	17.683	17.532	17.490
	0.053	0.050	0.045	0.047	0.044	0.047	0.051	0.056	0.063	0.060	0.078	0.073	0.099
34	17.760	17.595	17.607	17.528	17.522	17.529	17.460	17.458	17.388	17.361	17.235	17.182	16.959
	0.050	0.029	0.041	0.046	0.037	0.042	0.061	0.049	0.056	0.058	0.063	0.062	0.071
35	17.551	17.430	17.570	17.543	17.591	17.536	17.580	17.534	17.607	17.614	17.476	17.427	17.118
	0.042	0.043	0.046	0.064	0.051	0.060	0.069	0.070	0.083	0.080	0.087	0.083	0.086
36	18.239	18.061	18.089	18.000	17.994	17.909	17.946	17.787	17.741	17.761	17.677	17.527	17.364
	0.054	0.047	0.045	0.047	0.041	0.043	0.057	0.047	0.045	0.045	0.073	0.051	0.066
37	17.024	16.834	16.849	16.883	16.806	16.870	16.846	16.892	16.882	16.783	16.731	16.808	16.693
	0.016	0.014	0.014	0.016	0.013	0.015	0.016	0.019	0.023	0.024	0.032	0.030	0.047
38	18.172	17.882	17.887	17.894	17.686	17.731	17.577	17.669	17.577	17.448	17.367	17.229	17.409
	0.072	0.056	0.049	0.070	0.049	0.057	0.060	0.071	0.074	0.061	0.077	0.070	0.103
39	17.649	17.469	17.526	17.532	17.498	17.505	17.500	17.519	17.524	17.519	17.437	17.410	17.425
	0.035	0.035	0.033	0.043	0.032	0.037	0.037	0.045	0.052	0.051	0.066	0.060	0.077
40	16.911	16.752	16.811	16.797	16.818	16.801	16.811	16.802	16.816	16.825	16.735	16.791	16.695
	0.027	0.026	0.024	0.028	0.025	0.028	0.030	0.031	0.030	0.032	0.034	0.038	0.048
41	18.444	18.204	18.182	18.195	18.069	18.087	18.051	18.082	17.994	17.951	17.910	17.675	17.553
	0.134	0.132	0.114	0.168	0.112	0.128	0.134	0.152	0.157	0.141	0.163	0.126	0.142
43	18.005	17.758	17.852	17.747	17.771	17.735	17.712	17.673	17.681	17.726	17.796	17.584	17.574
	0.027	0.022	0.019	0.020	0.017	0.023	0.022	0.027	0.028	0.030	0.053	0.040	0.068
44	18.147	17.902	17.920	17.801	17.702	17.643	17.471	17.415	17.280	17.169	17.132	16.945	16.867
	0.060	0.060	0.057	0.064	0.059	0.063	0.055	0.063	0.061	0.052	0.068	0.050	0.063
45	18.066	17.704	17.638	17.515	17.354	17.315	17.210	17.183	17.119	17.062	17.006	16.977	16.851
	0.030	0.022	0.018	0.021	0.017	0.019	0.019	0.022	0.023	0.024	0.038	0.035	0.042
46	18.035	17.778	17.796	17.709	17.636	17.578	17.501	17.490	17.421	17.425	17.327	17.290	17.298
	0.037	0.030	0.026	0.028	0.024	0.024	0.026	0.030	0.036	0.030	0.048	0.044	0.065
49	18.987	18.374	18.294	17.948	17.893	17.679	17.445	17.368	17.167	17.186	17.164	16.998	16.925
	0.069	0.039	0.036	0.030	0.024	0.023	0.024	0.023	0.021	0.024	0.038	0.035	0.043
50	18.861	18.525	18.490	18.403	18.244	18.217	18.164	18.137	17.939	17.872	17.987	17.810	17.530
	0.082	0.064	0.054	0.060	0.046	0.050	0.056	0.058	0.056	0.054	0.085	0.066	0.071
52	16.732	16.424	16.339	16.110	16.036	15.937	15.829	15.725	15.774	15.731	15.760	15.605	15.696
	0.011	0.009	0.007	0.007	0.006	0.006	0.006	0.006	0.006	0.006	0.009	0.007	0.012
53	18.205	17.571	17.244	17.022	16.686	16.539	16.331	16.414	16.110	15.890	15.692	15.732	15.518
	0.032	0.019	0.014	0.014	0.010	0.011	0.010	0.012	0.010	0.009	0.011	0.010	0.013
54	17.522	17.254	17.314	17.150	17.105	17.086	17.005	17.023	16.997	16.861	16.825	16.758	16.648
	0.019	0.016	0.015	0.016	0.014	0.015	0.016	0.017	0.018	0.017	0.022	0.021	0.027
56	16.604	16.446	16.495	16.450	16.455	16.510	16.431	16.480	16.438	16.399	16.336	16.331	16.310
	0.011	0.009	0.009	0.009	0.008	0.009	0.009	0.010	0.010	0.010	0.014	0.013	0.019
57	18.165	17.679	17.472	17.278	17.053	16.872	16.722	16.642	16.530	16.440	16.357	16.214	16.196
	0.029	0.017	0.013	0.013	0.010	0.011	0.009	0.010	0.010	0.010	0.015	0.011	0.020

Using the Landolt standards, Zhou et al. (2001) presented the relations between the BATC intermediate-band system and $UBVRI$ broadband system using the catalogs of Landolt (1983, 1992) and Galadí-Enríquez et al. (2000). Two of the relations are

$$m_B = m_{04} + (0.2218 \pm 0.033)(m_{03} - m_{05}) + 0.0741 \pm 0.033, \quad (1)$$

$$m_V = m_{07} + (0.3233 \pm 0.019)(m_{06} - m_{08}) + 0.0590 \pm 0.010. \quad (2)$$

Using equations (1) and (2), we transformed the magnitudes of 41 star clusters in BATC03, BATC04 and BATC05 bands to their B magnitudes, and those in BATC06, BATC07 and BATC08 bands to their V magnitudes. The values of V (BATC) and $(B-V)$ (BATC) of these clusters are listed in Table 2.

Figure 2 displays, for the star clusters, their flux distribution in the 13 BATC filters. For convenience, the fluxes are plotted relative to the flux in the filter BATC08 ($\lambda = 6075$ Å). From this figure, we can see that cluster 7 has strong emission lines.

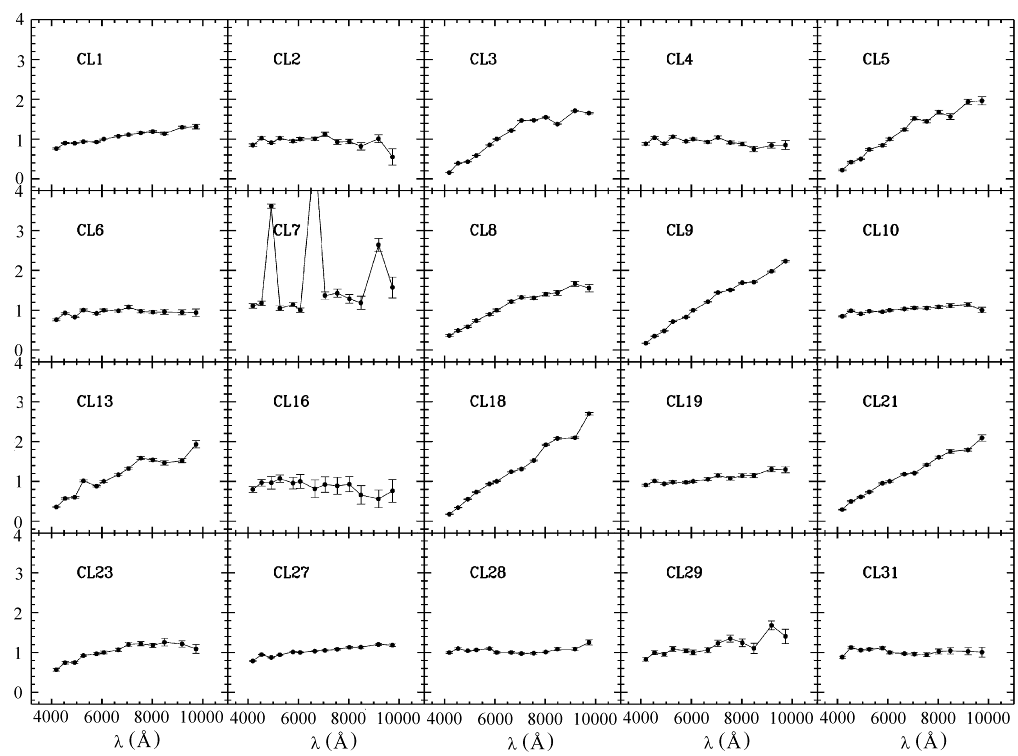

Fig. 2 Spectral energy distributions of 41 star clusters

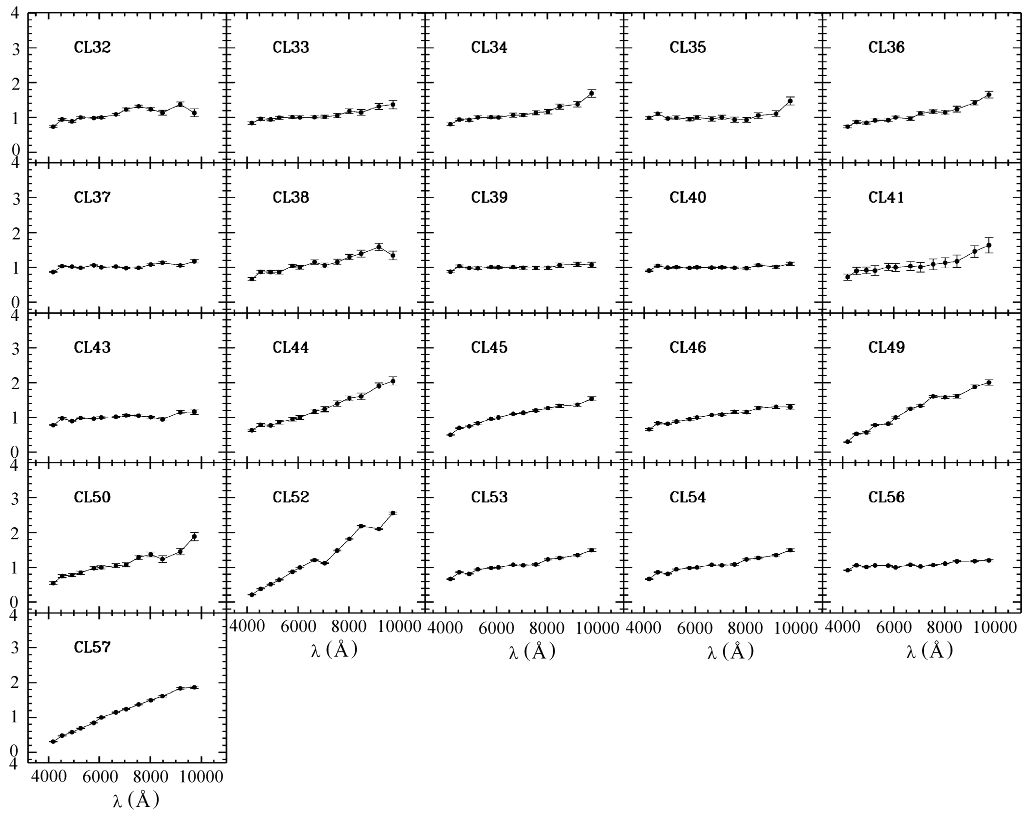

Fig. 2 Continued

3 SUMMARY

In this paper, we have, for the first time, obtained the SEDs of 41 star clusters of M33, that were detected by Melnick & D'odorico (1978). Our work can be summarized as follows.

1. Using the Beijing Astronomical Observatory 60/90 cm Schmidt Telescope we have obtained images of the 41 clusters in 13 intermediate-band filters from 3800 to 10 000 Å, and hence derived their spectral energy distributions.

2. The coordinates of these clusters were found from the HST Guide Star Catalog.

3. From the relations between the BATC intermediate-band system and $UBVRI$ broadband system, we have derived their V magnitudes and their $B-V$ colors. Most of the clusters are found to be blue.

Acknowledgements The BATC Survey is supported by the Chinese Academy of Sciences, the Chinese National Natural Science Foundation and the Ministry of Sciences and Technology of China. The project is also supported partly by the National Science Foundation (grant INT 93-01805) and by Arizona State University, the University of Arizona and Western Connecticut State University.

References

Barmby P., Huchra J. P., 2001, AJ, 122, 2458
Boulesteix J., Courtes G., Laval A., Petit H., 1974, A&A, 37, 33
Chandar R., Bianchi L., Ford H. C., 1999, ApJS, 122, 431
Chandar R., Bianchi L., Ford H. C., 2001, A&A, 366, 498
Christian C. A., Schommer R. A., 1982, ApJS, 49, 405
Fan X. H., Burstein D., Chen J. S. et al. 1996, AJ, 112, 628
Freedman W. L., Wilson C. D., Madore B. F., 1991, ApJ, 372, 455
Galadí-Enríquez D., Trullols E., Jordi C., 2000, A&AS, 146, 169
Landolt A. U., 1983, AJ, 88, 439
Landolt A. U., 1992, AJ, 104, 340
Ma J., Zhou X., Kong X. et al. 2001, AJ, 122, 1796
Ma J., Zhou X., Chen J. S. et al. 2002a, A&A, 385, 404
Ma J., Zhou X., Chen J. S. et al. 2002b, AJ, in press
Melnick J., D'Odorico S., 1978, A&AS, 34, 249
Sharov A. S., Lyutyi V. M., 1984, SvAL, 10, 273
Schommer R. A., Christian C. A., Caldwell N., Bothun G. D., Huchra J., 1991, AJ, 101, 873
Stetson P. B., 1987, PASP, 99, 191
Stetson P. B., 1992, PASP, 25, 297
Yan H. J., Burstein D., Fan X. H. et al. 2000, PASP, 112, 691
Zheng Z. Y., Shao Z. H., Su H. J. et al. 1999, AJ, 117, 2757
Zhou X., Jiang Z. J., Xue S. J. et al. 2001, CJAA, 1, 372
Zhou X., Jiang Z. J., Wu H. et al. 2002, in preparation